

# Transdermal Drug Delivery and Percutaneous Absorption: Mathematical Modeling Perspectives

Filippo de Monte<sup>a</sup>, Giuseppe Pontrelli<sup>b</sup>, Sid M. Becker<sup>c</sup>

<sup>a</sup>University of L'Aquila, L'Aquila, Italy

<sup>b</sup>Institute for Applied Mathematics—CNR, Rome, Italy

<sup>c</sup>University of Canterbury, Christchurch, New Zealand

## OUTLINE

10.1 Introduction	274	10.4 Modeling TDD Through a Two-Layered System	288
10.2 Physiological Description and Drug Transport Models	276	10.5 Conclusions	300
10.3 Review of Mathematical Methods	286		

## Nomenclature

- $c$  concentration ( $\text{kg m}^{-3}$ )  
 $C$  uniform initial concentration ( $\text{kg m}^{-3}$ )  
 $D$  effective diffusivity of the drug in the vehicle or skin ( $\text{m}^2 \text{s}^{-1}$ )  
 $J$  mass flux due to a concentration gradient ( $\text{kg s}^{-1} \text{m}^{-2}$ )  
 $k$  partition coefficient (dimensionless)  
 $k_p$  tissue permeability ( $\text{m s}^{-1}$ )  
 $K$  skin/capillary clearance coefficient ( $\text{m s}^{-1}$ )  
 $l$  thickness (m)  
 $M$  mass per unit of area ( $\text{kg m}^{-2}$ )  
 $P$  mass transfer coefficient ( $\text{m s}^{-1}$ )  
 $t$  time (s)

$x$  Cartesian space coordinate (m)

$X$  eigenfunction

## Greek Symbols

$\beta$  binding/unbinding rate constant ( $s^{-1}$ )

$\delta$  unbinding/binding rate constant ( $s^{-1}$ )

$\lambda$  eigenvalue

## Acronyms

PDE partial differential equation

SC stratum corneum

TDD transdermal drug delivery

TH theophylline

## Subscripts

0 unbound (free) drug in the vehicle

1 unbound (free) drug in the skin

b bound drug in the skin

e bound drug in the vehicle

## Superscripts

$k$  integer for series

## 10.1 INTRODUCTION

Systemic delivery of drugs by percutaneous permeation (transdermal drug delivery, TDD) offers several advantages compared to oral release or hypodermic injection. Because TDD's controlled release rate can provide a constant concentration for a long period of time and improved patient compliance, TDD has been shown to be an attractive alternative to oral administration [1]. The most advanced delivery systems (electroporation and cavitation ultrasound) enhance transdermal delivery through a strong and reversible disruption of the stratum corneum (SC), without damaging the deeper tissues.

Drugs can be delivered across the skin in order to have an effect on the tissues adjacent to the site of application (topical delivery) or to be effective after distribution through the circulatory system (systemic delivery). While there are many advantages to delivering drugs through the skin, the skin's barrier properties provide a significant challenge. To this aim, it is important to understand the mechanism of drug permeation from the delivery device (or vehicle, typically a transdermal patch or medicated plaster, as in Figure 10.1, or from novel delivery devices such as arrays of microneedles [2–5]).

Mathematical modeling for TDD constitutes a powerful predictive tool to arrive at a better understanding of the fundamental physics underlying biotransport processes. In the absence of experiments, many studies have used mathematical models and numerical simulations to research TDD efficacy and the optimal design of TDD devices [3,6,7]. The transdermal release

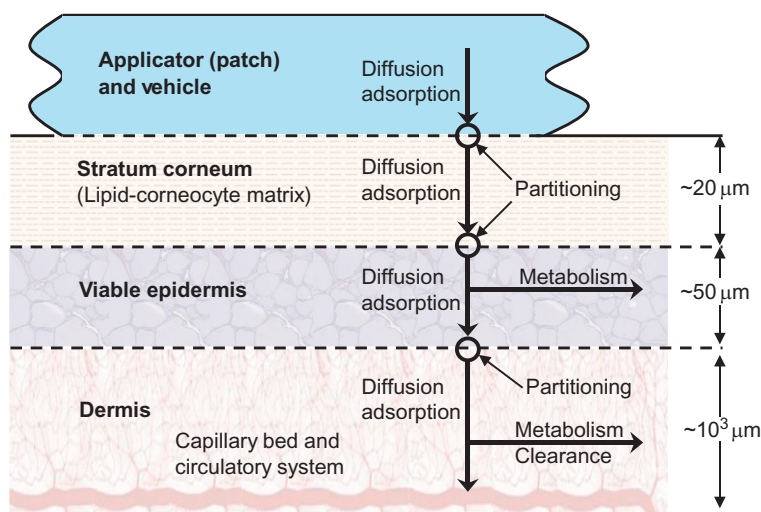


**FIGURE 10.1** The composite representation of the skin with an applicator for transdermal delivery. The layers are not drawn to scale and actual skin layer thicknesses can vary depending on the body site and on the individual. Transport mechanisms are listed as well.

of a drug must be carefully tailored to achieve the optimal therapeutic effect and to deliver the correct dose in the required time [8]. The pharmacological effects of the drug (the tissue accumulation, duration, and distribution) all have an effect on its efficacy. Hence, a delicate balance between an adequate amount of drug delivered over an extended period of time and the minimal local toxicity should be found [9]. Although a large number of mathematical models are available for drug dynamics in the skin, there is a limited effort to explain the drug delivery mechanism from the vehicle platform. This is a very important issue indeed, because the polymer matrix acts as a drug reservoir, and a strategic design of its microstructural characteristics would improve the release performances [10]. It is noteworthy to emphasize that the drug elution depends on the properties of the “vehicle-skin” system, taken as a whole, and can be modeled as a coupled two-layered system. In it, coupled to diffusive effects, drug binding and unbinding phenomena are considered. In both layers, these effects play an important role.

In Section 10.4 of this chapter a “vehicle-skin” coupled model is presented and a semianalytical form is given for drug concentration and mass within the vehicle and the skin at various times. Our mathematical approach is similar to that used to describe mass dynamics from a drug-eluting stent in an arterial wall and is similarly based on a two-layer diffusion model [11]. The simulations, aimed at the design of technologically advanced vehicles, can be used to provide valuable insights into local TDD and to assess experimental procedures to evaluate drug efficacy. A major issue in modeling drug penetration is the assessment of the key parameters defining skin permeability, diffusion coefficients, and partition coefficients. A big challenge is the large number of parameters required for an advanced modeling, which are often not readily available in the literature. With this in mind, we begin this chapter with a discussion of the physiological environment of the skin and its effect on the kinetics of drug transport.

## 10.2 PHYSIOLOGICAL DESCRIPTION AND DRUG TRANSPORT MODELS

This introductory section is written with a particular audience in mind—engineers and mathematicians unfamiliar with the terminology and basics of the field of dermal pharmacology. We have written this introduction with the intent of providing insight into the various parameters and constants that are so commonly used in the related mathematical models. The engineer or mathematician will find comfort in the familiar approach to the solutions of the transient conservative equations. However, when it comes to interpreting the results of a parametric analysis, this audience will be at a loss if they do not have a basic understanding of the meanings and the sources of the values representing the parametric constants. With this in mind, we begin this section with a general physiological description of the body's greatest organ, the skin. This is followed by a brief discussion of the considerations that must be made when approaching the modeling of transdermal transport. The descriptions and terminology are presented with the mathematical modeling perspective in mind so that the reader may more easily make the connection between mathematics, physics, and physiology.

### 10.2.1 The Skin as a Composite

The human skin is not a homogeneous medium as it is made of multiple constituent composite layers, each providing a specific function with varying thicknesses. The reader unfamiliar with the physiology of the skin may find the following texts helpful: the very comprehensive introductory book by Millington and Wilkinson [12] and the shorter, but highly informative synopsis by Wood and Bladon [13].

The outer skin layer, the epidermis (0.05-1.5 mm), is without vasculature and acts as a protective barrier preventing molecular transport. Below the epidermis is the highly vascular inner skin layer, the dermis (0.3-3 mm). An important characteristic of the dermis is the large network of capillaries with high blood flow rates exceeding several times that of metabolic requirements. The primary reason for such high perfusion rates in the dermis is to regulate body temperature: perfusion rates decrease in order to conserve body heat and increase in order to cool the body. The dermis is also characterized by its high collagen content, which provides the skin with its structural support. The skin, at most sites on the body, is perforated by appendages pathways in the form of sweat glands and hair follicles. Although such shunt routes occupy less than 0.1% of the lateral surface area of the skin, in some instances, they may contribute to electrically assisted diffusion transport [14]. In any model of *in vivo* skin (living, as in skin attached to a living body) that focuses on the kinetic response of a drug to the physiology of the skin, it is important to consider the adequacy of the model's composite layer and its physiological description of the skin.

### 10.2.2 The SC, Its Corneocytes, and the Lipid Matrix

The thin (10-50  $\mu\text{m}$ ) outermost layer of the epidermis is called the *stratum corneum*. This is the most resistive layer to transport through the skin. Although the SC's barrier function is vitally important to healthy skin (by keeping harmful molecules from passing into the skin and providing an initial defense against infection), it is this high resistance to permeability

that presents a major obstacle for successful transdermal delivery. Thus, in TDD modeling, a great deal of research is focused on the structure and the resulting barrier behavior of the SC.

At the sub-membrane scale, the SC is often described as a medium that is composed of two primary components: corneocytes, which are essentially flat, dead, keratinized cells and a lamellar network of lipid bilayers. The SC is composed of 15-20 layers of corneocytes which are interconnected by a lipid lamellar bilayer structure in a crystalline-gel phase [15,16]. The nature in which individual corneocytes are set within the lamellar matrix of lipid bilayers has inspired researchers to conceptualize a brick-and-mortar microstructure of the SC in which the corneocytes are represented by isolated bricks and the lipid structure is represented by a continuous mortar space encapsulating the bricks [15]. Individual SC corneocytes are 10-40  $\mu\text{m}$  in diameter, and they may differ in their thickness depending on the body site and their relative location within the SC. The corneocyte thickness may also be influenced by their degree of hydration, which varies from 10% to 30% bound water. Excellent descriptions of the understanding of the SC's microstructure are provided in Refs. [15,17]. The corneocytes and lipid structures have a strong contrast in their chemical behavior: the former are regarded as hydrophilic while the surrounding extracellular lipid matrix is lipophilic (water is lipophobic). With respect to TDD, a great deal of attention is focused upon the lipid regions of the SC. This is primarily because the drugs and drug vehicles have been designed such that they are lipophilic [15]. Lipophilic drugs will naturally prefer the lipid-filled spaces of the SC to the hydrophilic corneocytes, and thus transport circumventing the barrier function of the SC is primarily associated to occur within the lamellar lipid structure of the SC [16].

The molecular structure of the lipid phase has been well researched and publicized in various works by Bouwstra et al. [16,18,19] over the past two decades. The microstructure of the lipid phase is such that the lipid bilayers (heads and tails) are organized in a series of repeating periodic parallel sheets. The long periodicity phase has a periodicity of  $\sim 13$  nm and is believed to play a major role in the barrier function of the SC [18].

### 10.2.3 The Drug and the Vehicle

In describing the delivery of drugs, it is common to focus on the local concentration of the drug itself. However, in practice, the drug is not delivered to the skin in isolation. A transporting agent is used to administer the drug and to enhance the efficacy of delivery. Such an agent (termed the "vehicle") may serve several purposes in the transdermal delivery system. The vehicle in general is inert, having by itself no real therapeutic value. Transdermal delivery vehicles come in many forms such as colloids, creams, gels, lotions, ointments, liquids, and powders. When the vehicle is placed directly onto the skin surface, it acts as a medium to give the drug bulk and to provide the drug a contact time. In some applications, the vehicle can serve as a solvent in which the drug is dissolved. In more advanced cases, the vehicle is designed such that it encapsulates the drug on the journey through the SC [20]. Some such vehicles are designed with the chemical microstructure of the skin in mind so that the vehicle is more easily able to pass through the skin compared to the drug alone. An excellent review of penetration enhancers is provided by Williams and Barry [21]. With regards to the modeling of TDD, it is important to note that the drug's interaction with the vehicle must be considered. In the following section, some simple concepts will be described that allow for the drug vehicle interaction to be taken into account.

## 10.2.4 Diffusion–Transport Considerations

The structures of the skin (and of biological media in general) pose a number of unique phenomena that influence passive transport. The following is provided as a synopsis of the more detailed descriptions provided in Ref. [22] and which is summarized in the excellent recent reviews by Mitragotri et al. [3] and by Naegel et al. [23] and in the books of collected chapters by Roberts et al. [24,25]. For further insight, the reader is encouraged to consider the excellent historical review and fundamental description that is provided in the seminal work by Scheuplein and Blank [26]. The rate of distribution of a drug into the skin is dependent upon a number of critical factors associated with the skin's tissue layers. These include the tissue microstructure, the tendency for the drug or the drug's vehicle to become bound within this local microstructure, the drug's lipid or water solubility, the rates of metabolism within the tissue, and the rate of blood perfusion in the dermis.

### 10.2.4.1 Diffusion

In the absence of advection and electrokinetic effects, passive diffusion is responsible for the transport of a drug (solute) through the vehicle (solvent) and, then, through the skin layers. In its most general representation, for a mixture of two components (for example, drug and vehicle), the one-dimensional flux  $J$  per unit area (along  $x$ ) of drug transport by diffusion through the solvent follows Fick's law (also known as Fick's first law). Hence, it is directly proportional to the gradient in concentration  $c$ :

$$J = -D \frac{\partial c}{\partial x} \quad (10.1)$$

where  $D$  is the diffusion coefficient of the drug in the binary mixture, for example drug/vehicle.

When a steady-state condition is reached, the Fick's first law reduces to  $J_{SS} = \Delta c / (l/D)$ . It is important to recognize that steady state can only be reached after the lag time for solute diffusion has passed. The lag time for diffusion across a homogeneous membrane is given by  $l^2 / (6D)$ . It is noteworthy to mention that Higuchi [27] expressed Fick's first law more appropriately in terms of thermodynamic activity rather than the more widely used concentration approximation. Thermodynamic activity for any given solute is generally defined by the fractional solubility of the solute in the medium.

It is important to consider that a drug will have a different diffusion coefficient depending upon which vehicle or layer of skin that the drug is in. For example, the drug will have one associated diffusion coefficient in the SC and a different diffusion coefficient in the neighboring epidermis. Furthermore, at the macroscale within a specific layer, the tissue may be considered to be homogeneous, while at the microscale the medium is only periodically homogeneous. For example, at the macroscale, the SC will seem homogeneous, while, the SC is depicted as a matrix of corneocytes and lamellar structures of lipid bilayers.

Thus, the diffusion coefficient of Equation (10.1) is often an "effective" or "apparent" diffusion coefficient that represents the diffusional behavior of a drug in the tissue at a macroscale perspective. In order to apply a particular effective diffusion coefficient to a solute within a particular medium, the condition must be met that the time for equilibrium to be achieved at the microscale must be much shorter than the time required for transport across

the entire layer. This is not the case when the diffusion coefficient varies chemically (with concentration) [28] or if there are slow kinetic processes related to binding and unbinding [9]. This is further discussed in [Section 10.2.5](#).

By taking conservation of drug mass (see [Section 3.3](#) in de Monte et al. [29]), Equation (10.1) leads to the well-known one-dimensional, transient, diffusion equation (also known as Fick's second law):

$$\frac{\partial c}{\partial t} = D \frac{\partial^2 c}{\partial x^2} \quad (10.2)$$

where the calculation of the concentration distribution  $c = c(x, t)$  requires that the starting concentration as well as the conditions for concentration or flux at the boundaries (i.e., at the outermost and innermost surfaces) be specified: it requires the knowledge of the boundary and initial conditions. Therefore, different concentration solutions are obtained for different starting values of concentration and the boundary conditions.

#### 10.2.4.2 Evaluation of the Diffusion Coefficient

The evaluation of apparent diffusion coefficient values of various solutes in various vehicles and in the different skin layers (or in the skin as a whole) has been heavily researched with obvious motivation. However, it seems that the coefficient's value depends highly on the conditions used to approximate it. The evaluation of the diffusion coefficient requires multiscale and multiphysics considerations. Because the SC is the most rate-limiting layer to transdermal delivery, a great deal of attention has been given to evaluating the effective diffusivity within this layer alone.

There are two primary methods that have been used to estimate the diffusion coefficient that is related to steady-state conditions. One involves experimentally-obtained data of steady-state fluxes across a medium. A steady-state permeability,  $k_P$ , of the drug or carrier across a layer of thickness,  $l$ , is determined from the experimentally-measured steady-state flux,  $J_{SS}$ , and the difference in steady concentrations across the layer,  $\Delta c$ , as:

$$k_P = \frac{J_{SS}}{\Delta c} \quad (10.3)$$

Then, the diffusion coefficient may be determined from the relation:

$$D = k_P l \quad (10.4)$$

In the event that the drug is carried by a vehicle, the permeability and diffusion coefficient are related not only to the translayer diffusion of the drug itself, but are related also to the drug within the vehicle [25] by the relations:

$$k_P = \frac{J_{SS}}{\Delta c_V} \quad (10.5)$$

where  $c_V$  corresponds to the concentration of the solute within the vehicle.

Then, the diffusion coefficient may be determined from the relation:

$$D = k_{SV} k_P l \quad (10.6)$$

where  $k_{SV}$  corresponds to the partition coefficient of the solute between the skin and the vehicle (partitioning is discussed in the following [Section 10.2.4.3](#)).

There are limitations to the experimental approach. This is because the diffusion coefficient derived from the steady-state flux may not always accurately represent the behavior of transient diffusion. A second limitation to this method of evaluating the diffusion coefficient is that the conditions of any model that uses this value must have conditions that precisely match the experimental conditions from which the diffusion coefficient was evaluated.

This is the motivation of the second method of diffusion coefficient estimation, which involves model-based approximations. For example, the Potts-Guy model [30] describes the diffusion coefficient within the SC that is treated as an essentially homogeneous membrane. The diffusion coefficient is related to solute molecular weight in an exponentially decaying relationship [31]:

$$\frac{D_{SC}}{l_{SC}} = 10^{-6.3} e^{-0.0061 MW} \text{ cm s}^{-1} \quad (10.7)$$

where MW is the solute molecular weight. The predominant feature of this model (that even later, more complicated microstructure models retain) is the model's exponential dependence upon the solute volume (or molecular weight).

### 10.2.4.3 Partitioning

Partitioning is used to describe the behavior of a compound that is added to a binary mixture. When a solute is added to an isolated single-component system, it will arrange itself in a uniform concentration throughout the system. However, when this same solute is added into an isolated two-component system, the solute will arrange itself preferentially to one of the system components. To put this into context, consider a lipophilic solute that diffuses into a compartment that is filled with two components (A and B). If component A is lipophilic and component B is hydrophilic, the drug will prefer the environment occupied by lipophilic material A over that of hydrophilic material B. Thus, at steady state, a concentration will arise in which, taken separately and individually, A and B each have distinct and uniform concentrations of the drug, for which lipophilic section A will have a higher concentration than hydrophilic component B.

This concept is referred to as partitioning and can be derived from first principles perspectives as in Chapter 4 of Ref. [25] and in Chapter 5 of Ref. [32]. Following the derivations of Ref. [32], the partition coefficient may be defined as:

$$k_{AB} \equiv \frac{c_A}{c_B} \quad (10.8)$$

where  $c_A$  is the steady-state concentration of the drug in A and  $c_B$  is the steady-state concentration of the drug in B.

Equation (10.8) requires that the system be at thermal equilibrium (that the system be at a constant temperature). At the interface between component A and component B ( $x = x_{AB}$ ), at any time  $t$ , the partition coefficient is employed into an interface condition such that:

$$c_B(x_{AB}, t)k_{AB} = c_A(x_{AB}, t) \quad (10.9)$$

Partitioning in TDD is concerned with a drug's diffusive behavior at the interface between two different tissue types or microscopic regions. At the cellular level (microscale),

partitioning occurs within the SC at the interface between the lipids and the corneocytes, and between the drug's vehicle and the SC lipids. However, at the membrane level (macroscale), partitioning occurs at the layer interfaces (at the interfaces between the donor and the SC, between the SC and viable epidermis, between the epidermis and the dermis, etc.).

#### **10.2.4.4 Evaluation of the Partition Coefficient**

The dermal partition coefficients and dermal effective diffusion coefficients of 26 different compounds in mammalian dermis were examined and reported in an excellent work by Kretsos et al. [33]. Evaluating the partition coefficient between the SC and a vehicle is a very difficult task. The recent review of Mitragotri et al. [3] provides an excellent overview of the current methods that are employed to represent the partition coefficient within the SC. This review explains that the partitioning of the solute into the lipid bilayers is influenced by a chemical factor and a physical factor. The chemical factor accounts for the fact that the environment in the lipid bilayers is much more hydrophobic than its surroundings. The physical factor accounts for the actual molecular structure of the SC's arrangement of the lipid bilayers.

The field takes the view that "it is reasonable to assume that the partition coefficient of a solute from water into SC lipids is comparable to that into an isotropic solvent that reasonably mimics the SC lipid environment" [3]. For this reason, the reader will find that the partition coefficient of solutes in the literature is often reported in terms of the readily available octanol-water partition coefficient [34].

#### **10.2.5 Adsorption**

The concept of adsorption (sometimes referred to as binding/unbinding) of a drug or carrier into the local molecular microstructure has been extensively studied both experimentally and theoretically in various studies by Anissimov and Roberts [9,24,28,35,36]. In short, the concept can be conventionalized as follows.

On its route through the skin, a drug may encounter localized pockets (within the microstructure) that act to restrain the drug from transport. This is most often and most easily described within the SC. Consider the simple diffusion of water through the SC. Recalling that the lipid-filled spaces are lipophilic and the individual corneocytes are hydrophilic, it is not difficult to imagine that as a water molecule diffuses through the SC, it could become adsorbed into one of the corneocytes. Because the corneocyte shell provides a restrictive envelope through which the water is unable to freely diffuse, once the water is inside the corneocyte, it could be considered to be "bound" to remain within the space occupied by this individual corneocyte.

The adsorption is not restricted to occur within the corneocyte: defects within the SC lipid lamellar structures sometimes create small hydrophilic pockets within this otherwise lipophilic environment. At the molecular scale, individual drug molecules may bind to the corneocyte envelope. Furthermore, adsorption can take place outside of the SC. Consider the comprehensive discussion on the parameters associated within the dermis by Kretsos et al. [33]. There it is postulated that, in some instances, the solute can bind to large, relatively immobile macromolecules, such as proteins in the dermis. This, too, would constitute a binding process.

Mathematically, the binding and unbinding of a species (as it follows the path through the skin's layers) may be considered by categorizing the species into two subspecies: one representing the concentration of the drug in its unbound state,  $c_u$ , and the other representing the concentration of the drug in its bound state,  $c_b$ . The generalized description of adsorption, presented in a recent study by Nitsche and Frasch [37], comprehensively addresses the interpretation of this phenomenon from a macroscopic perspective, distinguishing between slow binding and fast binding.

### 10.2.5.1 Slow Binding

The development of the system of coupled partial differential equations (PDE's) representing this process was detailed by Anissimov and Roberts [9] in the context of the diffusion of water through the SC. The model provides a simple linear coupling between the bound ( $c_b$ ) and unbound ( $c_1$ ) states. The conservation of the solute mass in the unbound state is represented by:

$$\frac{\partial c_1}{\partial t} = D_1 \frac{\partial^2 c_1}{\partial x^2} - \beta_1 c_1 + \delta_1 c_b \quad (10.10)$$

Because it is not bound, it is free to diffuse spatially. Here the binding rate constant,  $\beta_1$ , provides a representation of the rate at which the solute leaves the free state and enters the bound state. The rate of release of bound drug into its unbound state is implied by the unbinding rate constant  $\delta_1$ . This linear representation of the exchange between the two states couples the concentration of the unbound state to that of the drug in its bound state:

$$\frac{\partial c_b}{\partial t} = \beta_1 c_1 - \delta_1 c_b \quad (10.11)$$

The binding and unbinding rate constants, that appear in Equations (10.10) and (10.11), have units of inverse time: their magnitudes are inversely proportional to the time associated with the binding/unbinding process. Equations (10.10) and (10.11) are used in cases of what is termed *slow binding*, that is, when the time scale associated with the binding process is not negligible when compared to the time scale associated with transport by diffusion. Thus, the rate constants associated with slow binding are small.

For water penetration through human SC, it was shown in Ref. [9] that  $\beta_1 \approx \delta_1 \approx 0.05 \text{ min}^{-1}$  ( $\approx 10^{-3} \text{ s}^{-1}$ ). According to Anissimov et al. [35], "It is reasonable to expect that, for larger molecules, binding constants will be much smaller."

The binding rates of theophylline (TH) in human skin were also evaluated experimentally in Ref. [38] and then explained by an extended partition-diffusion model with reversible binding. In the case of TH binding to keratin, the above study finds:  $\beta_1 = (0.466 \pm 0.147) \text{ h}^{-1}$ , i.e.,  $\beta_1 = (1.3 \pm 0.4) \times 10^{-4} \text{ s}^{-1}$ , and  $\beta_1/\delta_1 = 1.401$ . These values were subsequently used in the theoretical development study of Nitsche and Frasch [37].

### 10.2.5.2 Fast Binding

While the problem and solutions developed later in this chapter (Section 10.4) are related primarily to adsorption with slow binding/unbinding rates, for completeness, the development of the equations governing the fast binding rate case is provided as well. In the event

that the binding rate is very fast, that is, rate constants very large, the left hand side (LHS) of Equation (10.11) is negligible and so that the fast binding rate relation may be made:

$$\beta_1 c_1 = \delta_1 c_b \quad (10.12)$$

This directly relates the concentration of the bound state to the unbound state. Now consider that the total concentration  $\bar{c}_1$  may be defined as a sum of bound and unbound concentrations:

$$\bar{c}_1 = c_1 + c_b \quad (10.13)$$

and, furthermore, the conservation of the total solute mass is governed by:

$$\frac{\partial \bar{c}_1}{\partial t} = D_1 \frac{\partial^2 c_1}{\partial x^2} \quad (10.14)$$

When the relation Equation (10.12) is substituted into the definition Equation (10.13) and this in turn into the governing Equation (10.14), a single species representation of the transient diffusion may be made:

$$\frac{\partial}{\partial t} \left[ \left( 1 + \frac{\beta_1}{\delta_1} \right) c_1 \right] = D_1 \frac{\partial^2 c_1}{\partial x^2} \quad (10.15)$$

This simple representation of the fast binding adsorption processes has been developed and modified to capture nonlinear effects as well [39]. While the fast binding rate approximation allows for a simpler set of equations, it has been noted that the slow binding rate equations may be more representative of the local physics [23].

### 10.2.6 Metabolism and Clearance

The metabolic activity within the viable epidermis and the dermis may strongly influence the rate and delivery. Obviously, in some instances, the metabolism of the drug by the cells is, in itself, the motivation of the delivery: the targeted delivery cells are actively metabolizing the drug. The metabolic rate of the consumption of solute, having  $c$  as concentration, is generally represented by a simple sink term in a first-order reaction [23,40–42], that is  $-\mu_{ms}c$ , where  $\mu_{ms}$  is the metabolic rate constant ( $s^{-1}$ ).

The values of the rate constant are specific to the drug metabolized and the location within the skin. The works of Yamaguchi et al. provide values of the metabolic rate constants within the dermis for several specific drugs [40–42].

Clearance is similar to metabolism in that the effect of clearance is to remove solute from the tissue. This is most notably associated with the bulk removal of solute via the microcapillary system in the dermis. Recall that the dermis is highly perfused; it has rates of blood flow exceeding those of metabolic requirements. For a systemic delivery, the drug will be adsorbed into the dermal vasculature. The actual process of removal of solute from the dermis via the capillary system is complicated. It involves the diffusion of the solute from within the dermal interstitial space, through the capillary walls, and then by hydrodynamic means into the blood stream. An excellent description of this process is provided in the comprehensive review by Kretsos and Kasting [43] who include a compendium of experimentally derived data involving the parameters concerning capillary geometry and kinetics. In their 2004 work, Kretsos et al. [44] reduce the complexity of the representation of clearance within the dermis

by providing a simple term that (from a macroscale perspective) acts as a sink, so that within the dermis, the transient transport is represented by:

- slow binding (extension of Eq. (10.10))

$$\frac{\partial c_1}{\partial t} = D_1 \frac{\partial^2 c_1}{\partial x^2} - \beta_1 c_1 + \delta_1 c_b - \kappa_1 c_1 \quad (10.16a)$$

- fast binding (extension of Eq. (10.15))

$$\frac{\partial}{\partial t} \left[ \left( 1 + \frac{\beta_1}{\delta_1} \right) c_1 \right] = D_1 \frac{\partial^2 c_1}{\partial x^2} - \kappa_1 c_1 \quad (10.16b)$$

where the  $\kappa_1$  parameter ( $\text{s}^{-1}$ ) is the clearance coefficient, whose effects represent the removal of drug by the microvasculature system. In this study, experimental data of salicylic acid in de-epidermized rat skin is presented in order to develop an analytic approximation of the associated clearance. They report a clearance coefficient  $\kappa_1 = 9.1 \times 10^{-4} \text{ s}^{-1}$ .

While reducing the complexities of the dermal microvasculature to a single sink term may seem an oversimplification, it does provide information on the spatial behavior of the drug within the lower skin layers. Alternately, many reputable studies provide a further simplification of this phenomenon at the cost of this spatial information. In those studies, the dermal clearance behavior is represented by a boundary condition of the third kind at the dermis-epidermis interface:

$$K_1 c_1 + D_1 \frac{\partial c_1}{\partial x} = 0 \quad (10.17)$$

where  $K_1$  is the skin-capillary clearance having dimensions of velocity ( $\text{m s}^{-1}$ ) and related to the  $\kappa_1$  coefficient stated before by  $K_1 = \kappa_1 l_1$ , where  $l_1$  is the skin thickness.

### 10.2.7 TDD Models

Mathematical models of TDD and percutaneous absorption are highly relevant to the development of a fundamental understanding of biotransport processes as well as to the assessment of dermal exposure to industrial and environmental hazards. The foundations of predictive modeling of transdermal and topical delivery were laid in the 1940-1970s. During this time, it was recognized that partitioning and solubility were important factors that determine skin penetration.

This review summarizes the key developments in predictive simulation of skin permeation and related solution methods over the last 50 years and also looks to the future so that such approaches are effectively harnessed for the development of better topical and transdermal formulations and for improved assessment of skin exposure to toxic chemicals.

### 10.2.7.1 Fickian Models

Compartment models, also called pharmacokinetic (PK) models of skin, are often used to study the fate of chemicals entering and leaving the body. The PK models treat the skin and also the body as one or several well-stirred compartments of uniform (average) concentration that act as reactors and/or reservoirs of chemical storage with transfer between the compartments depicted by first order rate constant expressions. While permeation across the skin can be described using Equation (10.3), it is often represented in a PK model as either a series of compartments to mimic the partitioning and diffusion processes in the SC or as one compartment and two compartments that separately distinguish the lipophilic SC and hydrophilic viable epidermis layers of the skin [36].

While most attention in the field of modeling of skin permeation has been focused on describing diffusion processes in the SC, it has been recognized that additional processes including binding and metabolism [45] also play an important role in determining drug uptake. Binding is especially significant because many substances bind to keratin, which significantly influences their permeation across the SC.

The effect of binding on transdermal transport in the context of the epidermal penetration has been discussed by Roberts et al. [24] where the kinetics associated with the reservoir effect of the SC was considered. It was assumed in this work that binding is instantaneous, that is equilibration between bound and unbound states is fast compared to diffusion. The advantage of such an approach is that the modeling in this case is relatively simple with the diffusion coefficient  $D$  in the diffusion equation being replaced by an effective diffusion coefficient  $D_{\text{eff}}$ , where  $D_{\text{eff}} = f_u D$  and  $f_u$  is the fraction of unbound solute. As the fraction unbound is less than unity, binding leads to slower diffusion, and therefore longer lag times. If binding/partitioning is not fast compared to diffusion, the single diffusion equation has to be replaced by coupled PDE's [9], as shown in Section 10.2.5.1.

### 10.2.7.2 Non-Fickian Models

Often experimental results show that the predicted drug concentration distribution in the vehicle and in the skin by the Fick's model does not agree with experimental data. Recently, a non-Fickian mathematical model for the percutaneous absorption problem was proposed by Barbeiro and Ferreira [46].

In this new model, the Fick's law for the flux is modified by introducing a non-Fickian contribution defined with a relaxation parameter  $\tau_J$  related to the properties of the components. This parameter is similar to the relaxation time  $\tau_q$  of the heat flux for the analogous heat wave diffusion problem [47]. We have

$$J = -D \frac{\partial c}{\partial x} - \tau_J \frac{\partial J}{\partial t} \quad (10.18)$$

Combining the flux equation with the mass conservation law, a system of integro-differential equations was established with a compatibility condition on the boundary between the two components of the physical model. Alternatively, a hyperbolic PDE can be derived in place of the above integro-differential one, as done by Haji-Sheikh et al. [47]. In order to solve the mathematical model, its discrete version was introduced by Barbeiro

and Ferreira [46] and the demanding stability and convergence properties of the discrete system were studied by the analysis of numerical experiments.

### 10.3 REVIEW OF MATHEMATICAL METHODS

The expression of transport of a solute across a skin barrier membrane involves a number of steps and phases in a space and time variant process. The formal description of this process as a single equation is not straightforward, other than as one or more approximations in definition of the transport conditions or in presentation of the solutions. Here, we begin with the conventional Laplace transform analytical approach used to solve diffusion equations, move to numerical methods that allow variations in space and time in the transport process and various complexities to be better addressed.

#### 10.3.1 Laplace Transform

Laplace transform is an integral transformation that is used to solve ordinary and partial differential equations. Its application for solving diffusion problems has been described in the well-known book by Crank [48] and by Carslaw and Jaeger [49] and Özişik [50] for the analogous heat conduction problems.

The popularity of the Laplace transform in the skin literature has increased since the availability of scientific software (e.g. Scientist, MicroMath Scientific software, Matlab, Mathematica) that can invert from the Laplace domain to the time domain and allow regression to experimental data without the extra work of first deriving a functional representation of the Laplace solution inverted into the time domain. With this type of software, having the Laplace solution is virtually as good as having a solution written in terms of time. Anissimov and Roberts [9,27,51,52] have used the numerical inversion of Laplace transform solutions to the diffusion equation for simulations and data analysis of skin transport experiments.

One of the useful properties of the Laplace transform is that it can be used directly (without inversion to the time domain) to determine some parameters. In transport through skin for the case of a constant donor concentration, such parameters are the steady-state flux and the lag time [51,52].

While Laplace transforms offer numerous advantages in solving diffusion equations, they also suffer from certain limitations. Most notably, to be solvable by the Laplace transform, the partial differential equations must have concentration-independent coefficients. Also, the coefficients in the differential equation (e.g., the diffusivity in Equation (10.3)) have to be independent of time (e.g., constants or functions of space only) for the Laplace transform to convert the partial differential equation into an ordinary differential equation of  $x$  only. This excludes important classes of problems in skin transport that involve the diffusion coefficient changing with concentration (nonlinear equation) or with time; for example, co-diffusion with a penetration enhancer or a diffusion coefficient that changes due to skin drying.

### 10.3.2 Finite Difference Method

The finite difference approach to solving a differential equation or a system thereof involves replacing the differential equation with a set of difference equations that cover the requisite space and time [50, Chapter 12]. There are many variations to this theme, the sophistication of which depends upon the problem to be solved. The most common difference approximations are centered differences, equations centered in space at the location where the approximation is made; similarly, for the time variable. But backward and forward differences are possible, too.

Finite difference methods are particularly advantageous for potentially nonlinear systems with either simple geometry or periodic geometry. Much of the efficiency is lost for disordered structures. Relative to finite element methods (FEMs), finite difference methods can be much more efficient on periodic problems such as a regular brick-and-mortar SC structure. However, considerable skill is required to construct accurate approximations at boundaries and to implement an efficient variable mesh scheme. Relative to Laplace transform methods, the biggest advantages of finite differences are the ability to handle nonlinear problems and more complex boundary conditions; for instance, mixed boundary conditions. Both call for considerable skill by the operator.

### 10.3.3 Finite Element Method

The FEM is related to the finite difference method in that both offer approximate numerical solutions to linear or nonlinear PDE's. The FEM is able to handle domains with regular or irregular geometries and boundaries, including moving boundaries. The primary basis for the FEM is the discretization of a continuous domain of interest—here the skin—into a discrete set of connected subdomains. The resulting mesh of triangles or higher order polygons, referred to as elements, creates a finite-dimensional linear problem whose solution can be implemented on a computer. In general, the density of the mesh varies across the domain, with greater density over those areas where greater precision in the solution is required.

An example might be the regions in the SC near a boundary between corneocyte and lipid domains. Owing to the complexity of the meshing and solution procedures, the FEM is frequently implemented using commercial software packages. Rim et al. [10] developed a finite element model consisting of two isotropic materials with different diffusion and partition coefficients, connected by an interfacial flux. The two materials are intended to represent a dermal patch or reservoir containing a drug of interest, and the skin. Addition of a permeation enhancer creates a coupled two-component system with concentration-dependent diffusivities to account for interactions between drug and enhancer.

Frasch and Barbero [53] analyzed a finite element model of the SC lipid pathway to investigate effective path length and diffusional lag times in this path compared with a homogeneous membrane of the same thickness. This research group also presented a transcellular pathway model, whereby permeants are granted access to the corneocytes via a corneocyte-lipid partition coefficient and separate diffusivity within corneocytes compared with lipids. Results pointed to a transcellular pathway with preferential corneocyte partitioning as the likely diffusional path for hydrophiles.

A secondary result from these investigations was the observation that the complex disordered geometric representation of the SC could be reduced to a simple, rectangular, brick-and-mortar geometry with very similar results [54]. Furthermore, for many realistic combinations of corneocyte/lipid partitioning and diffusivity, the short vertical connections between bricks can be ignored and the problem can be reduced to a two-layer lipid-corneocyte laminate model. This configuration is a good representation for the transcellular path with preferential corneocyte partitioning. Thus, for many purposes, the complex geometrical arrangement of the SC can be reduced to a much simpler geometry for which simpler numerical algorithms, such as the finite difference method, can be applied. In fact, analytical solutions for steady-state flux and lag time have been published for the multilayer laminate model [48–50].

### 10.3.4 Finite Volume Method

Heisig et al. [55] used a related method, finite volumes, to solve both one-dimensional transient and steady-state transport of drugs through a biphasic brick-and-mortar model of SC with isotropic lipids and permeable, isotropic corneocytes. This work demonstrated the contributions of corneocyte alignment, relative phase diffusivity, and phase partitioning in the barrier properties of the SC. Subsequent extensions in both two-dimensional skin models have been described in [56,57], and the group has explored the role of drug binding to corneocyte elements on skin transport [58].

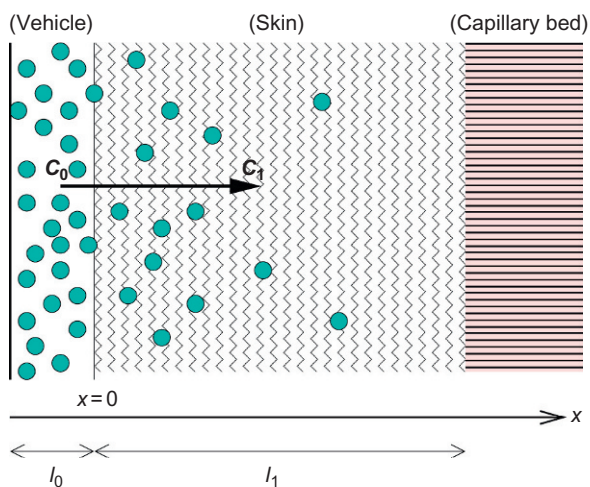
## 10.4 MODELING TDD THROUGH A TWO-LAYERED SYSTEM

In this section, we develop the governing equations and semianalytic solution to the problem of transport from a receiver vehicle into the skin. This approach attempts to capture the kinetics of the drug behavior in a one-dimensional transient domain. The various physiological considerations that were discussed in Section 10.2 are used to introduce the terms and parameters making up the associated PDE's. The general overview of the two-layer domain is such that the vehicle is represented by one layer (Layer 0) and all the constituent parts of the skin are lumped together into a second layer (Layer 1), as suggested by Kubota et al. [59] and by Simon and Loney [60]. This model will then consider partitioning, adsorption (binding), and diffusion of a drug as it passes from the vehicle (Layer 0) into the skin (Layer 1) and experiences clearance from the skin layer via the advection of the drug through the skin's micro-circulatory system. It is important for the reader to recognize that while the parameters used to represent the skin correspond in this model do not correspond to any individual layer of the skin, the physics that these parameters represent are those explained in Section 10.2.

### 10.4.1 Mathematical Formulation

Let us consider the two-layered delivery system. Layer 0 represents the vehicle by which the drug is administered for therapeutic purposes. The vehicle could be a transdermal patch or the film of an ointment placed directly onto the skin. Layer 1 represents the skin. In this

**FIGURE 10.2** Cross-section of the vehicle and the skin layers. Due to an initial difference of unbound concentrations  $c_0$  and  $c_1$ , a mass flux is established at the interface  $x=0$  and drug diffuses through the skin. At  $x=l_1$ , the skin-receptor (capillary) is set. Figure not to scale.



case, the skin of Layer 1 is representative of all the composite layers described in Section 10.2, the SC, the epidermis, and the dermis, and includes the dermal capillary bed. This is conceptualized in Figure 10.2. Because the lengths associated with the area of skin that is covered by the vehicle are very large compared to the lengths representing the skin and vehicle thicknesses, most of the mass dynamics occurs along the direction normal to the flat skin surface; so, we restrict our study to a simplified one-dimensional model. In particular, we consider the  $x$ -axis as normal to the skin surface and pointing outwards.

Without loss of generality, let  $x_0=0$  be the vehicle-skin interface; and  $l_0$  and  $l_1$  the thicknesses of these layers, respectively (Figure 10.2). Hence, both vehicle and skin are treated macroscopically as two homogeneous media. In this model, the governing equations of each layer (the vehicle and the skin) are developed such that the effects of binding and unbinding of each layer are considered. This means that in each layer (Layer 0 for vehicle and Layer 1 for skin) the drug can exist in a bound state and an unbound state. Thus, there are two equations for each layer that address the possible states of the drug.

The vehicle acts as a drug reservoir made of a thin substrate (generally, a polymer or a gel) containing a therapeutic drug to be delivered. Here, we will consider that initially within the vehicle, the entire mass of the drug exists in a bound state. This would be anticipated if the drug is encapsulated at maximum concentration in a solid phase of, for example, nanoparticles. In such a state, the drug cannot be delivered by diffusion into the skin, so it is considered “bound” and we denote the concentration of the drug within the vehicle that is bound by the symbol  $c_e$ . The vehicle is designed to release the drug from its solid bound state once it is applied to the skin. As the vehicle system starts the release process, a fraction of the drug mass is first transferred, in a finite time, to an unbound—free, biologically available—phase. In this model, the unbound drug within the vehicle is denoted  $c_0$ . The drug will then be available to diffuse into the skin. The drug enters the skin in an unbound state and, in this model, the concentration of the drug in Layer 1 (that is in the unbound state) is denoted  $c_1$ . Section 10.2.5 explained at the molecular level its route through the skin and the drug experience binding due to the local tissue microstructure. This model will consider that the drug may exist in the skin layer in a bound state as well. This is denoted by the symbol  $c_b$ .

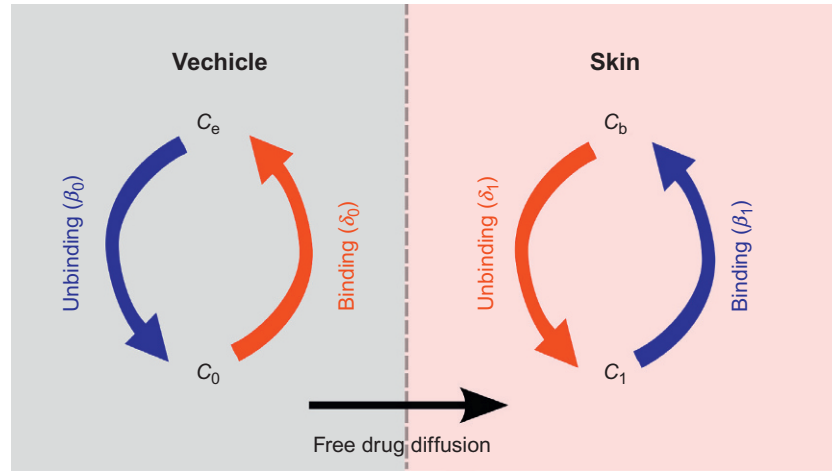


**FIGURE 10.3** Schematic of drug delivery and percutaneous absorption in the vehicle-skin system. An unbinding (resp. binding) reaction occurs in the vehicle (resp. in the skin). Reverse reactions are possible in both layers. Diffusion occurs only in the free unbound phases  $c_0$  and  $c_1$ .

Hence, the drug delivery process starts from the vehicle and ends at the skin receptors, with a phase change in a cascade sequence, as schematically represented in Figure 10.3. Bidirectional drug binding and unbinding phenomena play a key role in TDD, with characteristic times comparable (slow binding—Section 10.2.5.1) or faster (fast binding—Section 10.2.5.2) than those of diffusion.

Here we deal only with slow binding and will use the methods described in Section 10.2.5.1 in order to represent the kinetics of the drug in its bound state and its unbound state in both layers.

In Layer 0, the bound drug is governed by:

$$\frac{\partial c_e}{\partial t} = -\beta_0 c_e + \delta_0 c_0 \quad (-l_0 < x < 0; t > 0) \quad (10.19a)$$

where the parameters  $\beta_0 \geq 0$  and  $\delta_0 \geq 0$  are the unbinding and binding rate constants in the vehicle, respectively.

The unbound drug in the vehicle is governed by the coupled equation:

$$\frac{\partial c_0}{\partial t} = D_0 \frac{\partial^2 c_0}{\partial x^2} + \beta_0 c_e - \delta_0 c_0 \quad (-l_0 < x < 0; t > 0) \quad (10.19b)$$

where  $D_0$  is the effective diffusion coefficient of the unbound solute within the vehicle.

The drug's behavior within the skin is also represented by a diffusion process that includes the effects of slow binding. The drug in the skin that is in the unbound state is governed by:

$$\frac{\partial c_1}{\partial t} = D_1 \frac{\partial^2 c_1}{\partial x^2} - \beta_1 c_1 + \delta_1 c_b \quad (0 < x < l_1; t > 0) \quad (10.20a)$$

where  $D_1$  is the effective diffusivity coefficient of the unbound solute,  $\beta_1 \geq 0$  and  $\delta_1 \geq 0$  are the binding and unbinding rate constants in the skin, respectively.

$$\frac{\partial c_b}{\partial t} = \beta_1 c_1 - \delta_1 c_b \quad (0 < x < l_1; t > 0) \quad (10.20b)$$

To close the previous two-layered mass transfer system of Equations (10.19a), (10.19b), (10.20a), and (10.20b), a flux continuity condition and a jump in concentration (due to partitioning) must be assigned at the vehicle-skin interface:

$$D_0 \left( \frac{\partial c_0}{\partial x} \right)_{x=0} = D_1 \left( \frac{\partial c_1}{\partial x} \right)_{x=0} \quad (t > 0) \quad (10.21a)$$

$$c_0(0, t) = k_{01} c_1(0, t) \quad (t > 0) \quad (10.21b)$$

where  $k_{01}$  is the partition coefficient defined in Section 10.2.4 between Layer 0 and Layer 1.

However, as the interface condition Equation (10.21b) would be rigorously valid only for steady-state conditions, in the current treatment we prefer not to use it (contrary to what is generally done in the TDD field), but to deal with the following interface equation:

$$P[c_0(0, t) - c_1(0, t)] = -D_1 \left( \frac{\partial c_1}{\partial x} \right)_{x=0} \quad (t > 0) \quad (10.21c)$$

where  $P$  is a mass transfer coefficient which accounts for partitioning of the drug at the interface vehicle-skin.

In such a way, the concentration ratio  $c_0(0, t)/c_1(0, t)$  is not constant and equal to  $k_{01}$  at any time, as indicated by Equation (10.21b), but can change with the time. Also,  $P$  (whose value is unknown) can be related to the partition coefficient  $k_{01}$  (whose value can be taken experimentally, as described in Section 10.2.4) when a steady state is reached. In fact, Equation (10.21c) gives ( $t \rightarrow \infty$ ):

$$c_0(0, \infty) = c_1(0, \infty) \underbrace{\left[ 1 + \frac{J_{SS}}{P c_1(0, \infty)} \right]}_{k_{01}} = k_{01} c_1(0, \infty) \quad (10.22a)$$

where  $J_{SS}$  is the steady-state mass flux. Also, bearing in mind Equations (10.5) and (10.6), we can write

$$P = \frac{D_1}{k_{01}(k_{01} - 1)l_1} \quad (10.22b)$$

Then, no mass flux passes between the vehicle and the surrounding, and we impose a no-flux condition:

$$D_0 \left( \frac{\partial c_0}{\partial x} \right)_{x=-l_0} = 0 \quad (t > 0) \quad (10.23)$$

Also, a boundary condition has to be imposed at the skin-receptor (capillary bed) surface. At this point, the elimination of the drug by the capillary system follows a first-order kinetics (see Section 10.2.6):

$$-D_1 \left( \frac{\partial c_1}{\partial x} \right)_{x=l_1} = K_1 c_1(l_1, t) \quad (t > 0) \quad (10.24)$$

where  $K_1$  is the skin-capillary clearance per unit area.

Finally, the initial conditions are

$$c_e(x, 0) = C_e, \quad c_0(x, 0) = 0 \quad (-l_0 < x < 0) \quad (10.25a)$$

$$c_1(x, 0) = 0, \quad c_b(x, 0) = 0 \quad (0 < x < l_1) \quad (10.25b)$$

#### 10.4.1.1 Dimensionless Equations

To get easily computable quantities, all the variables and the parameters appearing in the governing equations listed previously are normalized as follows:

$$\begin{aligned} \tilde{x} &= \frac{x}{l_1}, \quad \tilde{l}_0 = \frac{l_0}{l_1}, \quad \tilde{t} = \frac{D_1 t}{l_1^2}, \quad \gamma_0 = \frac{D_0}{D_1}, \quad \phi = \frac{Pl_1}{D_1} \\ K &= \frac{K_1 l_1}{D_1}, \quad \tilde{c} = \frac{c}{C_e}, \quad \tilde{\beta} = \frac{\beta l_1^2}{D_1}, \quad \tilde{\delta} = \frac{\delta l_1^2}{D_1} \end{aligned} \quad (10.26)$$

By omitting the tilde for sake of simplicity, the mass transfer problem of the two-layered system of Figure 10.2 governed by Equations (10.19a)–(10.21a), (10.21c), (10.23)–(10.25b), can be rewritten in a dimensionless form as:

$$\frac{\partial c_e}{\partial t} = -\beta_0 c_e + \delta_0 c_0 \quad (-l_0 < x < 0; t > 0) \quad (10.27a)$$

$$\frac{\partial c_0}{\partial t} = \gamma_0 \frac{\partial^2 c_0}{\partial x^2} + \beta_0 c_e - \delta_0 c_0 \quad (-l_0 < x < 0; t > 0) \quad (10.27b)$$

$$\frac{\partial c_1}{\partial t} = \frac{\partial^2 c_1}{\partial x^2} - \beta_1 c_1 + \delta_1 c_b \quad (0 < x < 1; t > 0) \quad (10.27c)$$

$$\frac{\partial c_b}{\partial t} = \beta_1 c_1 - \delta_1 c_b \quad (0 < x < 1; t > 0) \quad (10.27d)$$

with the following inner and outer BCs:

$$\left( \frac{\partial c_0}{\partial x} \right)_{x=-l_0} = 0 \quad (t > 0) \quad (10.28a)$$

$$\gamma_0 \left( \frac{\partial c_0}{\partial x} \right)_{x=0} = \left( \frac{\partial c_1}{\partial x} \right)_{x=0} \quad (t > 0) \quad (10.28b)$$

$$\phi [c_0(0, t) - c_1(0, t)] = - \left( \frac{\partial c_1}{\partial x} \right)_{x=0} \quad (t > 0) \quad (10.28c)$$

$$\left( \frac{\partial c_1}{\partial x} \right)_{x=1} + K c_1(1, t) = 0 \quad (t > 0) \quad (10.28d)$$

supplemented with the initial conditions:

$$c_e(x, 0) = 1, \quad c_0(x, 0) = 0 \quad (-l_0 < x < 0) \quad (10.29a)$$

$$c_1(x, 0) = 0, \quad c_b(x, 0) = 0 \quad (0 < x < 1) \quad (10.29b)$$

## 10.4.2 Method of Solution

Preliminarily, by using the first of the two equations (10.29a), we note that the solution of the linear homogeneous ordinary differential equation (ODE) (10.27a) is

$$c_e(x, t) = \underbrace{\exp(-\beta_0 t)}_{c_e^*(t)} + \delta_0 \underbrace{\exp(-\beta_0 t) \int_0^t c_0(x, \tau) \exp(\beta_0 \tau) d\tau}_{c_e^{**}(x, t)} \quad (10.30)$$

Hence, it turns out that  $c_e$  can be expressed as a function of  $c_0$  and can be considered in two parts. The first part on the right hand side (RHS) of Equation (10.30) depends only on the time (exponentially) and is due to the initial drug concentration other than zero of the bound state within the vehicle. The other part depends on both space and time and is influenced by the boundary conditions (10.28a)–(10.28d) through  $c_0$ .

Similarly, from Equation (10.27d), by using the second of the two equations (10.29b),  $c_b$  can be expressed as a function of  $c_1$  as:

$$c_b(x, t) = \beta_1 \underbrace{\exp(-\delta_1 t) \int_0^t c_1(x, \tau) \exp(\delta_1 \tau) d\tau}_{c_b^{**}(x, t)} \quad (10.31)$$

where the part depending only on the time is absent due to the zero initial concentration of the unbound state within the vehicle.

Let us now find a solution for  $c_0$  and  $c_1$  by the separation-of-variables (SOV) method

$$c_0(x, t) = X_0(x)G(t), \quad c_1(x, t) = X_1(x)G(t) \quad (10.32)$$

As a consequence of Equations (10.30) and (10.31), the part of  $c_e$  and  $c_b$  depending on both space and time,  $c_e^{**}$  and  $c_b^{**}$ , respectively, can be separated by the same eigenvector set as:

$$c_e^{**}(x, t) = X_0(x)G_e(t), \quad c_b^{**}(x, t) = X_1(x)G_b(t) \quad (10.33)$$

Therefore, Equations (10.30) and (10.31) become

$$c_e(x, t) = \exp(-\beta_0 t) + X_0(x)G_e(t), \quad c_b(x, t) = X_1(x)G_b(t) \quad (10.34)$$

The time-dependent exponential term, appearing in the first of the two equations (10.34) and due to the only initial drug concentration other than zero, does not allow the SOV method to be applied. Then, for purposes of computation of the functions  $X_0(x)$ ,  $X_1(x)$ ,  $G_0(t)$ ,  $G_1(t)$ ,  $G_e(t)$ , and  $G_b(t)$ , we first neglect the initial drug concentration of the bound state and then, by means of appropriate constants, we will again account for it.

Thus, substituting Equations (10.32) and (10.34) in Equations (10.27a)–(10.27d) and neglecting the exponential term as said above gives

$$\frac{dG_e}{dt} = -\beta_0 G_e + \delta_0 G_0 \quad (10.35a)$$

$$\frac{1}{\gamma_0 G_0} \left[ \frac{dG_0}{dt} - (\beta_0 G_e - \delta_0 G_0) \right] = \frac{1}{X_0} \frac{d^2 X_0}{dx^2} = -\lambda_0^2 \quad (10.35b)$$

$$\frac{1}{G_1} \left[ \frac{dG_1}{dt} - (\delta_1 G_b - \beta_1 G_1) \right] = \frac{1}{X_1} \frac{d^2 X_1}{dx^2} = -\lambda_1^2 \quad (10.35c)$$

$$\frac{dG_b}{dt} = -\delta_1 G_b + \beta_1 G_1 \quad (10.35d)$$

where  $\lambda_0$  and  $\lambda_1$  are separation constants. In the following, they will be denoted as the eigenvalues of the vehicle and skin, respectively.

#### 10.4.2.1 Time-Dependent Solution

Two decoupled systems, each of two ordinary differential equations defined in the time domain, may be derived from Equations (10.35a)–(10.35d). In a matrix form, we have

$$\frac{d}{dt} \begin{pmatrix} G_e \\ G_0 \end{pmatrix} = \begin{pmatrix} -\beta_0 & \delta_0 \\ \beta_0 & -(\delta_0 + \gamma_0 \lambda_0^2) \end{pmatrix} \begin{pmatrix} G_e \\ G_0 \end{pmatrix} \quad (t > 0) \quad (10.36)$$

$$\frac{d}{dt} \begin{pmatrix} G_1 \\ G_b \end{pmatrix} = \begin{pmatrix} -(\beta_1 + \lambda_1^2) & \delta_1 \\ \beta_1 & -\delta_1 \end{pmatrix} \begin{pmatrix} G_1 \\ G_b \end{pmatrix} \quad (t > 0) \quad (10.37)$$

The general solution of the previous two systems is

$$G_e(t) = A_\mu^+ \left( \frac{\delta_0}{\beta_0 + \mu_+} \right) \exp(\mu_+ t) + A_\mu^- \left( \frac{\delta_0}{\beta_0 + \mu_-} \right) \exp(\mu_- t) \quad (10.38a)$$

$$G_0(t) = A_\mu^+ \exp(\mu_+ t) + A_\mu^- \exp(\mu_- t) \quad (10.38b)$$

$$G_1(t) = A_\nu^+ \exp(\nu_+ t) + A_\nu^- \exp(\nu_- t) \quad (10.39a)$$

$$G_b(t) = A_\nu^+ \left( \frac{\beta_1}{\delta_1 + \nu_+} \right) \exp(\nu_+ t) + A_\nu^- \left( \frac{\beta_1}{\delta_1 + \nu_-} \right) \exp(\nu_- t) \quad (10.39b)$$

where  $\mu_\pm$  and  $\nu_\pm$  may be taken as

$$\mu_\pm = \frac{-(\beta_0 + \delta_0 + \gamma_0 \lambda_0^2) \pm \sqrt{(\beta_0 + \delta_0 + \gamma_0 \lambda_0^2)^2 - 4\gamma_0 \beta_0 \lambda_0^2}}{2} \quad (10.40)$$

$$\nu_\pm = \frac{-(\beta_1 + \delta_1 + \lambda_1^2) \pm \sqrt{(\beta_1 + \delta_1 + \lambda_1^2)^2 - 4\delta_1 \lambda_1^2}}{2} \quad (10.41)$$

It is easily seen that  $\mu_\pm$  and  $\nu_\pm$  are both real and negative. In order to satisfy the interface conditions, Equations (10.28b) and (10.28c), we should have  $G_0(t) = G_1(t)$ , that is  $\mu_\pm = \nu_\pm$  and  $A_\mu^\pm = A_\nu^\pm$ .

#### 10.4.2.2 Space-Dependent Solution: The Eigenvalue Problem

Two ordinary differential equations defined in the space domain may be derived from Equations (10.35b) and (10.35c) as:

$$\frac{d^2 X_0}{dx^2} + \lambda_0^2 X_0 = 0 \quad (-l_0 < x < 0) \quad (10.42a)$$

$$\frac{d^2 X_1}{dx^2} + \lambda_1^2 X_1 = 0 \quad (0 < x < 1) \quad (10.42b)$$

They are coupled through the interface conditions, Equations (10.28b) and (10.28c). Then, substituting Equations (10.32) and (10.34) in Equations (10.28a)–(10.28d) and neglecting the exponential term appearing in the first of the two equations (10.34), as done in Subsection 10.4.2, we have

$$\left( \frac{dX_0}{dx} \right)_{x=-l_0} = 0 \quad (10.42c)$$

$$\gamma_0 \left( \frac{dX_0}{dx} \right)_{x=0} = \left( \frac{dX_1}{dx} \right)_{x=0} \quad (10.42d)$$

$$\phi[X_0(0, t) - X_1(0, t)] = - \left( \frac{dX_1}{dx} \right)_{x=0} \quad (10.42e)$$

$$\left( \frac{dX_1}{dx} \right)_{x=1} + KX_1(1, t) = 0 \quad (10.42f)$$

Equations (10.42a)–(10.42f) represent a Sturm-Liouville (eigenvalue) problem with discontinuous coefficients whose solution is

$$X_0(x) = a_0 \cos(\lambda_0 x) + b_0 \sin(\lambda_0 x) \quad (-l_0 < x < 0) \quad (10.43a)$$

$$X_1(x) = a_1 \cos(\lambda_1 x) + b_1 \sin(\lambda_1 x) \quad (0 < x < 1) \quad (10.43b)$$

with

$$a_0 = - \left[ \frac{\lambda_1}{\phi} + \frac{K \tan(\lambda_1) + \lambda_1}{K - \lambda_1 \tan(\lambda_1)} \right] \quad (10.44a)$$

$$b_0 = \frac{1}{\gamma_0} \frac{\lambda_1}{\lambda_0} \quad (10.44b)$$

$$a_1 = - \frac{K \tan(\lambda_1) + \lambda_1}{K - \lambda_1 \tan(\lambda_1)} \quad (10.44c)$$

For  $K \rightarrow \infty$ , we have a boundary condition of the first kind at  $x = 1$  and Equations (10.44a)–(10.44c) reduce to the same equations as given in de Monte et al. [29, p. 100].

The eigencondition for computing the eigenvalues is  $a_0 \tan(\lambda_0 l_0) + b_0 = 0$ . Substituting the coefficients  $a_0$  and  $b_0$  listed before gives

$$\underbrace{\left[ \frac{\lambda_1}{\phi} + \frac{K \tan(\lambda_1) + \lambda_1}{K - \lambda_1 \tan(\lambda_1)} \right]}_{-a_0} \tan(\lambda_0 l_0) - \underbrace{\frac{1}{\sqrt{\gamma_0}} \frac{\lambda_1}{\sqrt{\lambda_1^2 + (\beta_1 - \delta_0)}}}_{b_0} = 0 \quad (10.45)$$

where the eigenvalues  $\lambda_0$  and  $\lambda_1$  are related through the constraint  $\mu_{\pm} = \nu_{\pm}$ , as shown in the previous paragraph, where  $\mu_{\pm}$  and  $\nu_{\pm}$  are given by Equations (10.40) and (10.41), respectively.

### 10.4.2.3 Concentration Solution

By numerically solving the transcendental equation (10.45) along with the condition  $\mu_{\pm} = \nu_{\pm}$ , an infinite set of real and distinct eigenvalues is computed, that is,  $\lambda_0^k$  and  $\lambda_1^k$ , with  $k=1, 2, \dots$ . Correspondingly, we will have a countable set of eigenfunctions  $X_0^k$  and  $X_1^k$ , defined through Equations (10.43a) and (10.43b), and of time-dependent functions  $G_e^k(t)$ ,  $G_0^k(t)$ ,  $G_1^k(t)$ , and  $G_b^k(t)$ , defined through Equations (10.38a) and (10.39b), respectively, with  $\mu_{\pm}^k = \nu_{\pm}^k$ .

Finally, the general solution will be given by the linear superposition of the fundamental solution in the form:

$$c_e(x, t) = \sum_{k=1}^{\infty} X_0^k(x) \left[ A_k \left( \frac{\delta_0}{\beta_0 + \mu_+^k} \right) \exp(\mu_+^k t) + B_k \left( \frac{\delta_0}{\beta_0 + \mu_-^k} \right) \exp(\mu_-^k t) \right] \quad (10.46a)$$

$$c_0(x, t) = \sum_{k=1}^{\infty} X_0^k(x) [A_k \exp(\mu_+^k t) + B_k \exp(\mu_-^k t)] \quad (10.46b)$$

$$c_1(x, t) = \sum_{k=1}^{\infty} X_1^k(x) [A_k \exp(\mu_+^k t) + B_k \exp(\mu_-^k t)] \quad (10.46c)$$

$$c_b(x, t) = \sum_{k=1}^{\infty} X_1^k(x) \left[ A_k \left( \frac{\beta_1}{\delta_1 + \mu_+^k} \right) \exp(\mu_+^k t) + B_k \left( \frac{\beta_1}{\delta_1 + \mu_-^k} \right) \exp(\mu_-^k t) \right] \quad (10.46d)$$

Bearing in mind the initial conditions  $c_0(x, 0) = 0$  and  $c_1(x, 0) = 0$ , it follows that  $B_k = -A_k$ , where  $A_k$  may be computed by using the remaining initial conditions, that is,  $c_e(x, 0) = 1$  and  $c_b(x, 0) = 0$ . In detail, we have

$$\sum_{k=1}^{\infty} A_k X_0^k(x) \left( \frac{\delta_0}{\beta_0 + \mu_+^k} - \frac{\delta_0}{\beta_0 + \mu_-^k} \right) = 1 \quad (-l_0 < x < 0) \quad (10.47a)$$

$$\sum_{k=1}^{\infty} A_k X_1^k(x) \left( \frac{\beta_1}{\delta_1 + \mu_+^k} - \frac{\beta_1}{\delta_1 + \mu_-^k} \right) = 0 \quad (0 < x < 1) \quad (10.47b)$$

By truncating the above two series to  $N$  terms and, then, by collocating in  $K$  points, the system of algebraic equations (10.47a) and (10.47b) is solved to get the constants  $A_k$ , with  $k=1, 2, \dots, N$ .

Then, the analytical form of the solution given by Equations (10.46a)–(10.46d) allows us an easy computation of the dimensionless drug mass (per unit of area),  $\tilde{M} = M / (C_e l_1) \rightarrow M$ , as an integral of the concentration over the correspondent layer, that is,

$$M(t) = \int c(x, t) dx \quad (0 < x < 1) \quad (10.48)$$

### 10.4.3 Numerical Simulation and Results

A common difficulty in modeling physiological processes is the identification of reliable estimates of the model parameters. Experiments of TDD are prohibitively expensive or impossible *in vivo* and the only available sources are data from literature. The physical problem depends on a large number of parameters; each of them may vary in a finite range, with a variety of combinations and limiting cases. Also, we develop the solution for a particular combination of parameters, that is  $\beta_0 = \delta_1$  and  $\beta_1 = \delta_0$ , being the general case addressed in Ref. [61]. Consequently, as  $\mu_{\pm}^k = \nu_{\pm}^k$ , we have:  $\gamma_0(\lambda_0^k)^2 = (\lambda_1^k)^2$ .

The physical parameter-values used are related to a beta-adrenoceptor blocking agent, timolol, released from the acrylic copolymer to local circulation through the skin. These parameter-values are given by [59,60]

- vehicle

$$D_0 = 2.7 \times 10^{-9} \text{ cm}^2 \text{ s}^{-1}, \quad l_0 = 40 \mu\text{m} \quad (10.49a)$$

- skin

$$D_1 = 7.8 \times 10^{-10} \text{ cm}^2 \text{ s}^{-1}, \quad l_1 = 125 \mu\text{m}, \quad K_1 = 3.5 \times 10^{-3} \text{ cm s}^{-1} \quad (10.49b)$$

- vehicle-skin interface

$$k_{01} = 1 \Rightarrow P \rightarrow \infty \quad (10.49c)$$

Equation (10.49c) states that there is no concentration jump at the interface as the partition coefficient is equal to 1. Therefore, the boundary condition expressed by Equation (10.21c) simply reduces to  $c_0(0, t) = c_1(0, t)$  for any  $t > 0$ .

As the binding/unbinding processes are not considered in Refs. [59,60], the corresponding reaction rates  $\beta_1 = \delta_0$  and  $\beta_0 = \delta_1$  are unavailable. However, as the characteristic reaction times are smaller than the diffusion times, in the current case (timolol in human skin) we can write (in dimensional form):  $\beta_1, \delta_1 > D_1/l_1^2 = 5 \times 10^{-6} \text{ s}^{-1}$ . Also, according to Anissimov et al. [35] it is reasonable to expect that, for larger molecules (such as timolol), binding/unbinding constants are smaller than the ones for water penetration through human SC where  $\beta_1 \approx \delta_1 \approx 10^{-3} \text{ s}^{-1}$  [9], as already shown in Section 10.2.5.1. Therefore, we have the following constraint for timolol through human skin:

$$5 \times 10^{-6} \text{ s}^{-1} < \beta_1, \quad \delta_1 < 10^{-3} \text{ s}^{-1} \quad (10.50)$$

In all numerical experiments, we have assumed:  $\beta_1 = \delta_0 = 10^{-4} \text{ s}^{-1}$  (the same order of TH binding to keratin) and three different values for  $\beta_0 = \delta_1$ . In detail:  $8 \times 10^{-5} \text{ s}^{-1}$ ,  $2 \times 10^{-4} \text{ s}^{-1}$ , and  $10^{-3} \text{ s}^{-1}$ , as shown in Figures 10.4–10.7 to follow.

Then, the limit of the skin layer ( $l_1$ ) was estimated by the following considerations. Strictly speaking, in a diffusion-reaction problem the concentration vanishes asymptotically at infinite distance. However, for computational purposes, the concentration is damped out (within a given tolerance) over a finite distance at a given time. Such a distance, known as “penetration distance”  $d_p$  [62], may be defined as the distance from the perturbed region at which

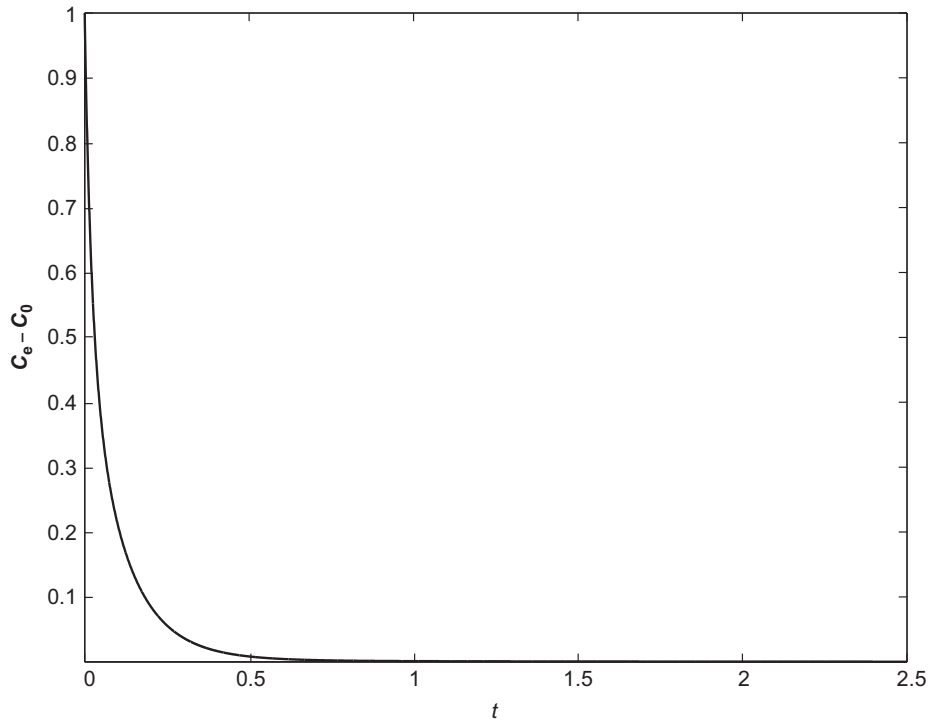


**FIGURE 10.4** Difference between bound and free concentrations,  $c_e - c_0$ , in the vehicle as a function of time for various locations.

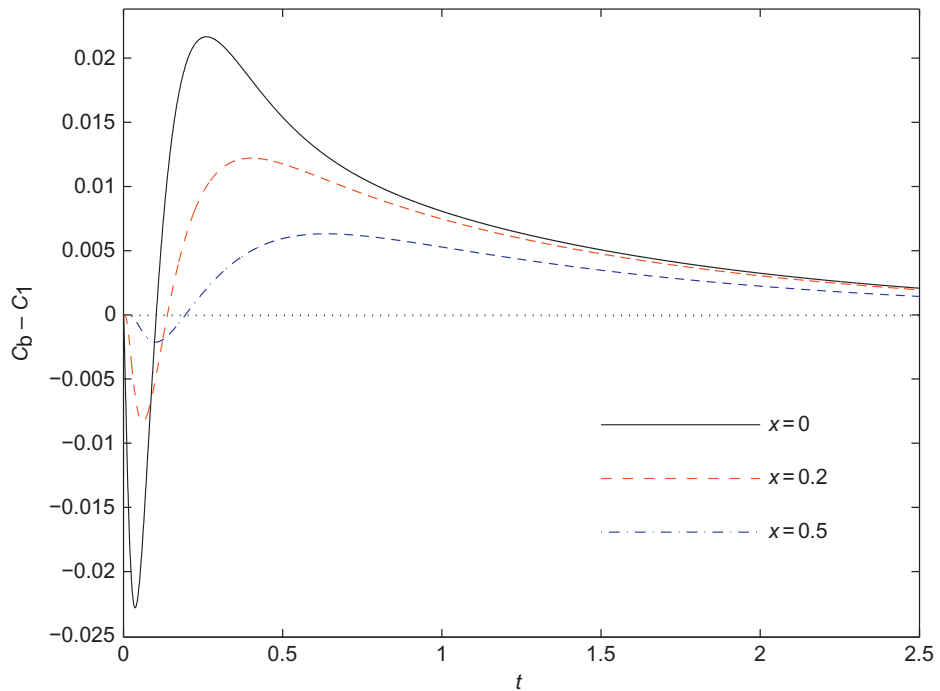


**FIGURE 10.5** Difference between bound and free concentrations,  $c_b - c_1$ , in the skin versus time with location as a parameter.

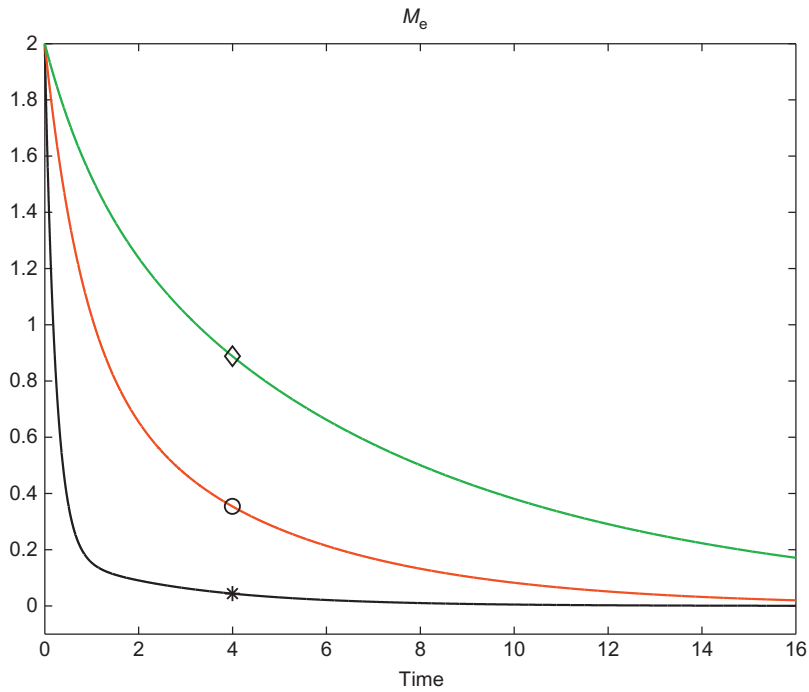


**FIGURE 10.6** Bound drug mass  $M_e$  in the vehicle versus time for  $\delta_0(=\beta_1)=10^{-4} \text{ s}^{-1}$  and three different values of the unbinding rate  $\beta_0=\delta_1(\text{s}^{-1})$ .

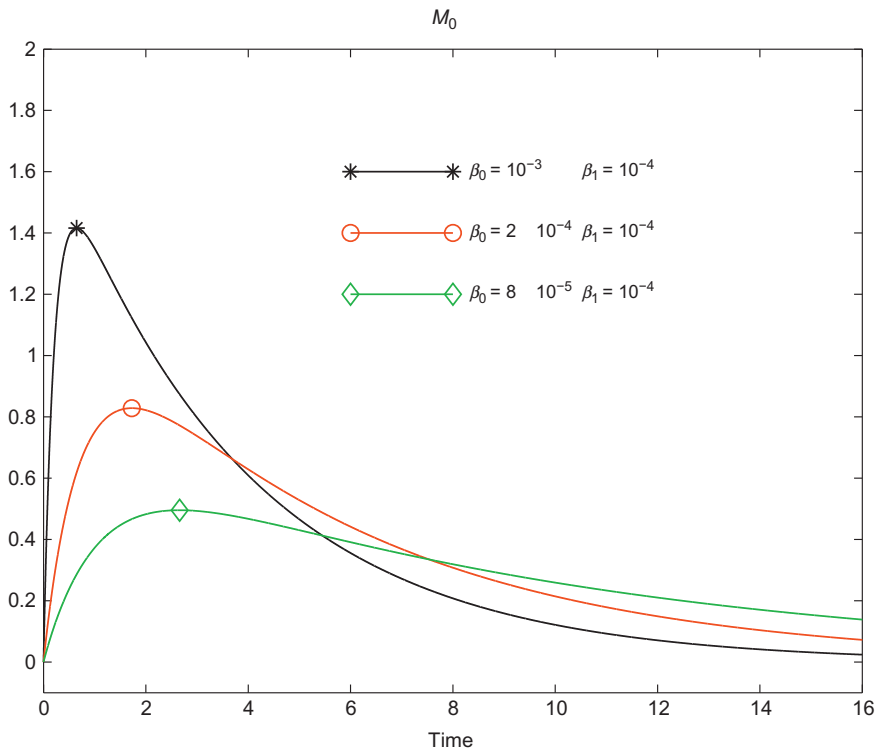


**FIGURE 10.7** Unbound drug mass  $M_0$  in the vehicle as a function of time for  $\delta_0(=\beta_1)=10^{-4} \text{ s}^{-1}$  with  $\beta_0=\delta_1(\text{s}^{-1})$  as a parameter.

concentration and mass flux are just affected (errors less than  $10^{-n}$ ;  $n=1,2,\dots,10$ ) at a given time  $t$  by this perturbation (in the current case, the initial condition  $c_e(x,0)=1$ ). It critically depends on the diffusive properties of both layers; in particular, it is related to the ratio  $\gamma_0=D_0/D_1$  as follows [63]

$$d_p \cong \begin{cases} \sqrt{10n\gamma_0 t}, & 0 \leq t \leq 0.1 l_0^2/(n\gamma_0) \\ \sqrt{10nt} + l_0 \left( \frac{\sqrt{\gamma_0} - 1}{\sqrt{\gamma_0}} \right), & t \geq 0.1 l_0^2/(n\gamma_0) \end{cases} \quad (10.51)$$

where  $d_p$  is dimensionless ( $d_p \rightarrow \tilde{d}_p = d_p/l_1$ )

Therefore, the outer boundary condition Equation (10.28d) may be replaced with

$$\begin{cases} c_1(x=0,t)=0, & 0 \leq t \leq 0.1 l_0^2/(n\gamma_0) \\ c_1(x=d_p,t)=0, & t \geq 0.1 l_0^2/(n\gamma_0) \end{cases} \quad (10.52)$$

where the first of the two prior equations states that, at early times  $0 \leq t \leq 0.1 l_0^2/(n\gamma_0)$ , the two-layer (vehicle/SC) system reduces to only one single layer (vehicle) slab with a homogeneous boundary condition of the first kind, that is,  $c_1(x=0,t)=0$ , with errors less than  $10^{-n}$  ( $n=1, 2, \dots, 10$ ).

The concentration is decreasing inside each layer, and vanishes at a distance that is within the SC, at all times. Due to the relatively large value of  $D_0$  and to the small value of  $l_0$ , the concentration profiles are almost flat in the vehicle, with levels reduced in time, and have a decreasing behavior in the skin layer. In particular, a fast decaying phase transfer is evidenced in the vehicle (Figure 10.4), whereas a fast phase change of drug occurs at early times within the skin, that is more evident at points close to the interface  $x=0$ , and continues at later times (Figure 10.5).

The mass  $M_e(t)$  exponentially decreases in the vehicle, as shown in Figure 10.6, while the mass  $M_0(t)$  first increases up to some upper bound and then decays asymptotically, as shown in Figure 10.7.

The relative size of  $\beta_0=\delta_1$  and  $\beta_1=\delta_0$  affects the binding/unbinding transfer processes, thus influencing the mechanism of the whole dynamics. The occurrence and the magnitude of the drug peak depend on the combination and the relative extent of the diffusive and reaction parameters. The outcome of the simulation provides valuable indicators to assess whether drug reaches target tissue and, hence, to optimize the dose capacity in the vehicle. For example, Figures 10.8 and 10.9 show that a lower value of the unbinding parameter  $\beta_0=\delta_1$  guarantees a more prolonged and uniform release. For the other way around, a large value of  $\beta_0=\delta_1$  is responsible for a localized peaked distribution followed by a faster decay.

The present TDD model constitutes a simple tool that can help in designing and in manufacturing new vehicle platforms that guarantee the optimal release for an extended period of time.

## 10.5 CONCLUSIONS

In the last decades, transdermal delivery has emerged as an attractive alternative and an efficient route for drug administration. After a general phenomenological description of the skin and its parameters, and a brief review of the main predictive modeling techniques and

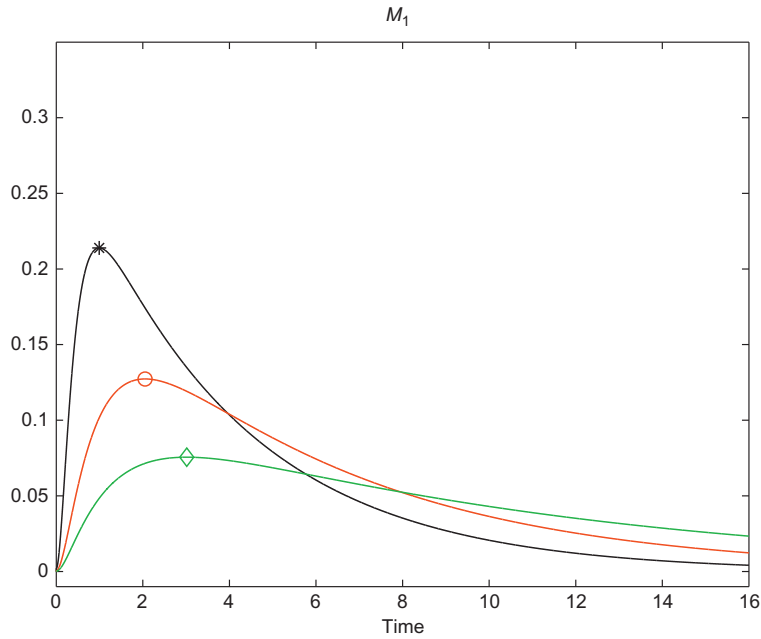


**FIGURE 10.8** Time history of the unbound drug mass  $M_1$  in the skin for  $\beta_1(=\delta_0)=10^{-4} \text{ s}^{-1}$  and three values of the unbinding rate  $\delta_1=\beta_0(\text{s}^{-1})$ .

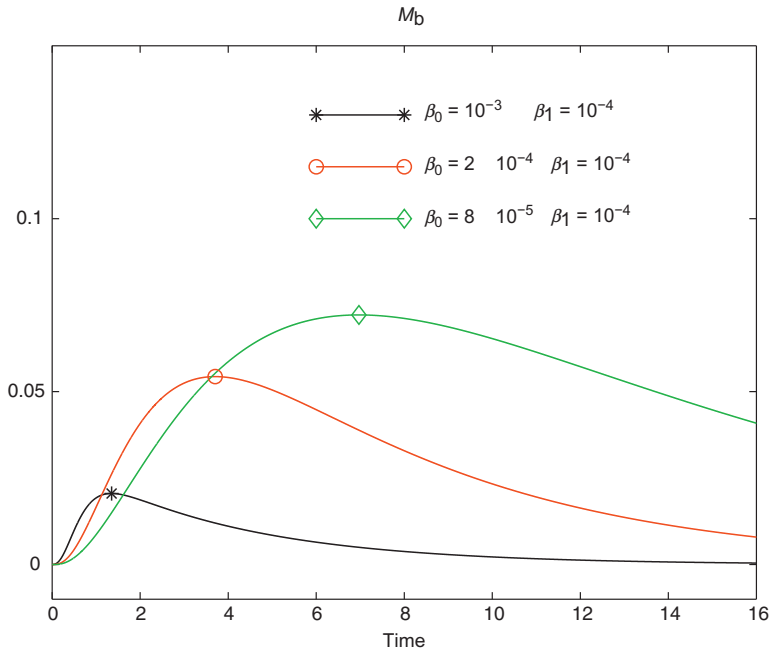


**FIGURE 10.9** Time plot of the bound drug mass  $M_b$  in the skin for  $\beta_1(=\delta_0)=10^{-4} \text{ s}^{-1}$  with  $\delta_1=\beta_0(\text{s}^{-1})$  as a parameter.

related analytical and numerical solutions, a comprehensive mathematical model of drug delivery by percutaneous permeation is presented in this chapter. To account for diffusion and reaction aspects of drug dynamics from the vehicle across the skin, a multiphase, two-layered model is developed and an eigenvalue-based semianalytic solution for drug concentration is proposed.

The model incorporates the reversible binding process and can be employed to study the effects of the various parameters that control the vehicle-skin delivery system. This can be of interest in the design of smarter devices in order to get the optimal therapeutic effect by releasing the correct dose in the required time. Although limited to a simple one-dimensional case, the results of the numerical simulations can offer a useful tool to estimate the performance of the drug delivery systems.

## References

- [1] Chien YW. Novel drug delivery systems. New York: Marcel Dekker; 1992.
- [2] Cevc G, Vierl U. Nanotechnology and the transdermal route: a state of the art review and critical appraisal. *J Control Release* 2010;141:277–99.
- [3] Mitragotri S, Anissimov YG, Bunge AL, Frasch HF, Guy RH, Hadgraft J, et al. Mathematical models of skin permeability: an overview. *Int J Pharm* 2011;418:115–29.
- [4] George K, Kubota K, Twizell E. A two-dimensional mathematical model of percutaneous drug absorption. *BioMed Eng* 2004;3:567–78.
- [5] Barry BW. Novel mechanisms and devices to enable successful transdermal drug delivery. *Eur J Pharm Sci* 2001;14:101–14.
- [6] Manitz R, Lucht W, Strehmel K, Weiner R, Neubert R. On mathematical modeling of dermal and transdermal drug delivery. *J Pharm Sci* 1998;87:873–9.
- [7] Addick W, Flynn G, Weiner N, Curl R. A mathematical model to describe drug release from thin topical applications. *Int J Pharm* 1989;56:243–8.
- [8] Prausnitz M, Langer R. Transdermal drug delivery. *Nat Biotechnol* 2008;26:1261–8.
- [9] Anissimov YG, Roberts MS. Diffusion modelling of percutaneous absorption kinetics: 4. Effects of a slow equilibration process within stratum corneum on absorption and desorption kinetics. *J Pharm Sci* 2009;98:772–81.
- [10] Rim JE, Pinsky P, van Osdol W. Finite element modeling of coupled diffusion with partitioning in transdermal drug delivery. *Ann Biomed Eng* 2005;33:1422–38.
- [11] Pontrelli G, de Monte F. Mass diffusion through two-layer porous media: an application to the drug-eluting stent. *Int J Het Mass Tran* 2007;50:3658–69.
- [12] Millington PF, Wilkinson R. *Skin*. Cambridge: Cambridge University Press; 2009.
- [13] Wood EJ, Bladon PT. *The human skin*. London: Edward Arnold; 1985.
- [14] Barry BW. Drug delivery routes in skin: a novel approach. *Adv Drug Deliv Rev* 2002;54(Suppl. 1):S31–40.
- [15] Menon GK. New insights into skin structure: scratching the surface. *Adv Drug Deliv Rev* 2002;54(Suppl. 1):S3–S17.
- [16] Bouwstra JA, Gooris GS. The lipid organization in human stratum corneum and model systems. *Open Derm J* 2010;4:10–3.
- [17] Madison KC. Barrier function of the skin: "La raison d'être" of the epidermis. *J Invest Dermatol* 2003;121:231–41.
- [18] Bouwstra JA, Gooris GS, van der Spek JA, Bras W. Structural investigations of human stratum corneum by small-angle X-ray scattering. *J Invest Dermatol* 1991;97:1005–12.
- [19] Bouwstra JA, Dubbelaar F, Gooris GS, Ponc M. The lipid organisation in the skin barrier. *Acta Derm Venereol* 2000;208:23–30.
- [20] Han IH, Choi SU, Nam DY, Park YM, Kang MJ, Kang KH, et al. Identification and assessment of permeability enhancing vehicles for transdermal delivery of glucosamine hydrochloride. *Arch Pharm Res* 2010;33:293–9.
- [21] Williams AC, Barry BW. Penetration enhancers. *Adv Drug Deliv Rev* 2004;56:603–18.
- [22] Barry BW. Modern methods of promoting drug absorption through the skin. *Mol Aspects Med* 1991;12:195–241.

- [23] Naegel A, Heisig M, Wittum G. Detailed modeling of skin penetration—an overview. *Adv Drug Deliv Rev* 2013;65:191–207.
- [24] Roberts MS, Pellett MA, Cross SE. Basic mathematical principles in skin permeation. In: Keith RB, Adam CW, editors. *Dermatological and transdermal formulations*. Boca Raton: CRC Press; 2002.
- [25] Roberts MS, Pellett MA, Cross SE. Skin transport. In: Walters KA, editor. *Dermatological and transdermal formulations*. Boca Raton: CRC Press; 2002.
- [26] Scheuplein RJ, Blank IH. Permeability of the skin. *Physiol Rev* 1971;51:702–47.
- [27] Higuchi T. Physical chemical analysis of percutaneous absorption process from creams and ointments. *J Soc Cosmet Chem* 1960;11:85–97.
- [28] Anissimov YG, Roberts MS. Diffusion modeling of percutaneous absorption kinetics: 3. Variable diffusion and partition coefficients, consequences for stratum corneum depth profiles and desorption kinetics. *J Pharm Sci* 2004;93:470–87.
- [29] de Monte F, Pontrelli G, Becker SM. Drug release in biological tissues. In: Becker SM, Kuznetsov AV, editors. *Transport in biological media*. 1st ed. New York: Elsevier Publishing; 2013. p. 59–118 [chapter 3].
- [30] Potts RO, Guy RH. Predicting skin permeability. *Pharm Res* 1992;9:663–9.
- [31] Kumins CA, Kwei TK. Free volume and other theories. In: Crank J, Park GS, editors. *Diffusion in polymers*. New York: Academic Press; 1968. p. 107–25.
- [32] Streng WH. Partition coefficient. In: Streng WH, editor. *Characterization of compounds in solution (Theory and Practice)*. USA: Springer; 2001. p. 47–60.
- [33] Kretsos K, Miller MA, Zamora-Estrada G, Kasting GB. Partitioning, diffusivity and clearance of skin permeants in mammalian dermis. *Int J Pharm* 2008;346:64–79.
- [34] Johnson ME, Berk DA, Blankschtein D, Golan DE, Jain RK, Langer RS. Lateral diffusion of small compounds in human stratum corneum and model lipid bilayer systems. *Biophys J* 1996;71:2656–68.
- [35] Anissimov YG, Jepps OG, Dancik Y, Roberts MS. Mathematical and pharmacokinetic modelling of epidermal and dermal transport processes. *Adv Drug Deliv Rev* 2013;65:169–90.
- [36] Roberts MS, Anissimov YG. Mathematical models in percutaneous absorption. In: Bronaugh RL, Maibach HI, editors. *Percutaneous absorption drugs—cosmetics—mechanisms—methodology*. 4th ed. New York: Marcel Dekker; 2005. p. 1–44.
- [37] Nitsche JM, Frasch HF. Dynamics of diffusion with reversible binding in microscopically heterogeneous membranes: general theory and applications to dermal penetration. *Chem Eng Sci* 2011;66:2019–41.
- [38] Frasch HF, Barbero AM, Hettick JM, Nitsche JM. Tissue binding affects the kinetics of theophylline diffusion through the stratum corneum barrier layer of skin. *J Pharm Sci* 2011;100:2989–95.
- [39] Kubota K, Twizell EH. A nonlinear numerical model of percutaneous drug absorption. *Math Biosci* 1992;108:157–78.
- [40] Yamaguchi K, Mitsui T, Yamamoto T, Shiokawa R, Nomiya Y, Ohishi N, et al. Analysis of in vitro skin permeation of 22-oxacalcitriol having a complicated metabolic pathway. *Pharm Res* 2006;23:680–8.
- [41] Yamaguchi K, Mitsui T, Aso Y, Sugibayashi K. Analysis of in vitro skin permeation of 22-oxacalcitriol from ointments based on a two- or three-layer diffusion model considering diffusivity in a vehicle. *Int J Pharm* 2007;336:310–8.
- [42] Yamaguchi K, Morita K, Mitsui T, Aso Y, Sugibayashi K. Skin permeation and metabolism of a new antipsoriatic vitamin D3 analogue of structure 16-en-22-oxa-24-carboalkoxide with low calcemic effect. *Int J Pharm* 2008;353:105–12.
- [43] Kretsos K, Kasting GB. Dermal capillary clearance: physiology and modeling. *Skin Pharmacol Physiol* 2005;18:55–74.
- [44] Kretsos K, Kasting GB, Nitsche JM. Distributed diffusion-clearance model for transient drug distribution within the skin. *J Pharm Sci* 2004;93:2820–35.
- [45] Liu P, Higuchi WI, Ghanem AH, Good WR. Transport of beta-estradiol in freshly excised human skin in vitro: diffusion and metabolism in each skin layer. *Pharm Res* 1994;11:1777–84.
- [46] Barbeiro S, Ferreira JA. Coupled vehicle-skin models for drug release. *Comput Method Appl M* 2009;198:2078–86.
- [47] Haji-Sheikh A, de Monte F, Beck JV. Temperature solutions in thin films using thermal wave Green's function solution equation. *Int J Heat Mass Tran* 2013;62:78–86.
- [48] Crank J. *The mathematics of diffusion*. 2nd ed. Oxford: Clarendon Press; 1979.

- [49] Carslaw HS, Jaeger JC. Conduction of heat in solids. 2nd ed. Oxford: Oxford University Press; 1959.
- [50] Özişik MN. Heat conduction. 2nd ed. New York: John Wiley & Sons; 1993.
- [51] Anissimov YG, Roberts MS. Diffusion modeling of percutaneous absorption kinetics: 1. Effects of flow rate, receptor sampling rate and viable epidermal resistance for a constant donor concentration. *J Pharm Sci* 1999;88:1201–9.
- [52] Anissimov YG, Roberts MS. Diffusion modeling of percutaneous absorption kinetics: 2. Finite vehicle volume and solvent deposited solids. *J Pharm Sci* 2001;90:504–20.
- [53] Frasch HF, Barbero AM. Steady-state flux and lag time in the stratum corneum lipid pathway: results from finite element models. *J Pharm Sci* 2003;92:2196–207.
- [54] Barbero AM, Frasch HF. Modeling of diffusion with partitioning in stratum corneum using a finite element model. *Ann Biomed Eng* 2005;33:1281–92.
- [55] Heisig M, Lieckfeldt R, Wittum G, Mazurkevich G, Lee G. Non steady-state descriptions of drug permeation through stratum corneum. I. The biphasic brick-and-mortar mode. *Pharm Res* 1996;13:421–6.
- [56] Naegel A, Hansen S, Newmann D, Lehr CM, Schaefer UF, Wittum G, et al. Insilico model of skin penetration based on experimentally determined input parameters. Part II: mathematical modelling of in vitro diffusion experiments, identification of critical input parameters. *Eur J Pharm Biopharm* 2008;68:368–79.
- [57] Naegel A, Heisig M, Wittum G. A comparison of two- and three-dimensional models for the simulation of the permeability of human stratum corneum. *Eur J Pharm Biopharm* 2009;72:332–8.
- [58] Hansen S, Naegel A, Heisig M, Wittum G, Neumann D, Kostka KH, et al. The role of corneocytes in skin transport revised—a combined computational and experimental approach. *Pharm Res* 2009;26:1379–97.
- [59] Kubota K, Dey F, Matar S, Twizell E. A repeated dose model of percutaneous drug absorption. *Appl Math Model* 2002;26:529–44.
- [60] Simon L, Loney N. An analytical solution for percutaneous drug absorption: application and removal of the vehicle. *Math Biosci* 2005;197:119–39.
- [61] Pontrelli G, de Monte F. A two-phase two-layer model for transdermal drug delivery and percutaneous absorption. *Math Biosci* 2014 (February) <http://dx.doi.org/10.1016/j.mbs.2014.05.001> [available online 14.05.14], in press.
- [62] de Monte F, Beck JV, Amos DE. Diffusion of thermal disturbances in two-dimensional Cartesian transient heat conduction. *Int J Heat Mass Tran* 2008;51:5931–41.
- [63] Pontrelli G, de Monte F. A multi-layer porous wall model for coronary drug-eluting stents. *Int J Heat Mass Tran* 2010;53:629–3637.